Laminar-Turbulent Transition Modelling in High Speed Flows

Jean-Philippe Brazier, Jean Perraud

Laminar-Turbulent Transition Modelling in High Speed Flows

Jean-Philippe Brazier[1], *Jean Perraud*[2]

Abstract

Predicting the position of the laminar-turbulent transition in high-speed boundary-layer flows is mandatory to estimate some key parameters such as the skin friction and the wall heat flux or the efficiency of a control surface. Linear stability theory has been used for many years to describe the amplification of small upstream fluctuations, which can be related to the transition position. Computational tools are developed to address more complex flow stability problems at higher velocities. However, some low-order models are still needed to give an estimation of transition location in RANS computations, on smooth surfaces as well as for localized indentations such as steps or gaps. Such models originally derived for low speed flows are progressively extended to higher Mach numbers.

Keywords: *laminar-turbulent transition, boundary-layer stability, hypersonic flows*

Nomenclature

Latin

A – wave amplitude
C_f – friction coefficient
M – Mach number
N – amplification factor
R – Reynolds number
T – temperature (K)
U – streamwise mean velocity ($m.s^{-1}$)
V – normal mean velocity ($m.s^{-1}$)
W – crosswise mean velocity ($m.s^{-1}$)
f – frequency (Hz)
p – pressure (Pa)
q – vector eigenfunction
t – time (s)
u – streamwise velocity fluctuation ($m.s^{-1}$)
v – normal velocity fluctuation ($m.s^{-1}$)
w – crosswise velocity fluctuation ($m.s^{-1}$)
x – streamwise coordinate (m)
y – normal coordinate (m)
z – crosswise coordinate (m)

Greek

Λ_2 – Pohlhausen parameter
α – axial wave number (m^{-1})
β – transverse wave number (m^{-1})
δ_1 – displacement thickness (m)
μ – dynamic viscosity (Pl)
θ – momentum thickness (m)
ρ – density ($kg.m^{-3}$)
ψ – wave vector angle (deg.)
ω – angular frequency (s^{-1})

Superscripts

$\bar{}$ – mean value
$'$ – fluctuating value

Subscripts

e – value at the boundary layer edge
i – imaginary part
r – real part
w – wall value
0 – initial value

1. Introduction

The laminar-turbulent transition of the boundary layer induces a strong increase in the skin friction and the wall heat flux, which are of key importance for hypersonic flows. Indeed, estimating the

[1] *ONERA, Toulouse University, France, Jean-Philippe.Brazier@onera.fr*
[2] *ONERA, retired*

maximum heat flux encountered during an atmospheric re-entry is mandatory to design the correct thermal protection system. An oversized thermal protection induces a useless mass increase and a consequent payload decrease. Moreover, the laminar-turbulent transition can modify the shock-wave/boundary-layer interaction occurring on a control surface hinge and thus change its efficiency for flight control.

On smooth surfaces, the laminar-turbulent transition is mainly due to the intrinsic instability of the boundary layer, inducing the exponential amplification of small fluctuations occurring in the oncoming flow, due to the natural atmospheric turbulence. As long as the amplitude of the perturbations remains low, they can be described by the linearized Navier-Stokes equations. When the amplitude of these fluctuations reaches a given threshold, nonlinear phenomena arise and they trigger very quickly the transition. The purpose of the flow stability analysis consists in computing an estimation of the global amplification of the perturbations in the boundary layer, most often characterized by the exponential amplification coefficient known as "the N factor". In the frame of the well-known e^N theory, the transition location is estimated at the position where the N factor reaches a prescribed value N_T, which depends on the free flow turbulence level. In flight, a value of 10 is frequently observed for N_T, whereas lower values around 6-7 can be encountered in low-speed low-noise wind tunnels and even values as low as 1 in noisy blow-down hypersonic facilities. Quiet hypersonic wind tunnels have been specifically designed to reproduce flight Mach number, Reynolds number and N_T. Only in these special facilities the mechanisms of laminar-turbulent transition can be similar to that occurring in flight.

The purpose of this paper is to present some recent works carried out at ONERA concerning the laminar-turbulent transition modelling. Whereas boundary-layer stability analysis can provide valuable information about the transition location, this approach is not easy to couple with a RANS computation. Therefore, some transition criteria have been developed for several decades for this purpose. On a smooth wall, they are derived by synthesizing stability results for a family of self-similar boundary-layer profiles, created by varying some characteristic parameters such as the Mach number and the streamwise pressure gradient. The stability of any boundary-layer profile can then be estimated from the model according to the values of the corresponding parameters. The effect of surface defaults on the transition location can also be modelled from a series of stability calculations, for different flow conditions past different geometries of defaults. In this paper, we will focus on the effect of transverse gaps.

The next section presents the different linear stability computation tools that have been developed up to now at ONERA or are intended for the near future. Section 3 is devoted to transition criteria on a smooth surface, to be included in RANS solvers. Then the last section 4 concerns the modelling of the influence of a transverse gap on the transition location.

2. Linear stability analysis tools

2.1. Common features

A set of computational tools for linear stability analysis has been developed for many years at ONERA Toulouse centre. Beside the legacy code *CASTET* developed by D. Arnal for local linear stability analysis of boundary layers, a new generation of solvers has emerged, adapted to various geometries and flow conditions. These solvers use similar internal architectures. For all of them, the linearized equations are derived with the appropriate hypotheses with the computational algebra software *Maple*. The elementary matrices corresponding to the linear equations at the current point are then directly transferred in the Fortran 2000 code. The numerical discretization schemes are also derived in the same manner. In this way, the risk of term omission or algebraic error is minimized. Some reference solutions can also be numerically computed directly with *Maple* in order to validate the whole Fortran code. The main matrix operations such as eigenvalue computations are carried out by standard linear algebra libraries such as *Lapack* or *Arpack*.

The first step to get the linearized Navier-Stokes equations consists in splitting all the variables into a time averaged value and a fluctuating part:

$$q(x,y,z,t) = \bar{q}(x,y,z) + q'(x,y,z,t) \quad (1)$$

where q represents any flow variable such as velocity component, enthalpy, pressure or density. Then, for modal analysis, a Fourier transform is applied on the time variable:

$$q'(x,y,z,t) = \tilde{q}(x,y,z)e^{-i\omega t}$$

where ω is the angular frequency. The next steps will consist in applying further simplifications to the equations, taking advantage of the hypotheses on the problem.

2.2. Local linear stability analysis

The basic case for stability analysis concerns a boundary layer with slow evolution in the streamwise and crosswise directions and strong variation only along the normal coordinate. Then the perturbation can be sought for under the form of a one-dimensional normal mode at a prescribed frequency:

$$q'(x,y,z,t) = \hat{q}(y)\exp[i(\alpha x + \beta z - \omega t)] \quad (2)$$

where α and β are respectively the streamwise and crosswise wave numbers. The angle ψ of the wave vector with the *x* axis is defined such as β = α tan(ψ). This approach will be named LST-1D, since only *y*-derivatives are retained in the equations. Usually, ω and β are real and prescribed whereas α is complex and unknown. The imaginary part of α represents the streamwise growth rate of the perturbation. After discretization of the differential equations along the normal *y* coordinate, the linearized Navier-Stokes equations can be recast in a generalized eigenvalue problem for α:

$$A.X = \alpha B.X \quad (3)$$

where X is the vector containing all the discretized eigenfunctions $[\hat{u},\hat{v},\hat{w},\hat{p},\hat{T}]$ and A and B are square matrices depending of β, ω, and the mean flow. When α is computed at each streamwise abscissa, the N factor can be derived as

$$N = \ln\frac{A(x)}{A_0} = \int_0^x -\alpha_i\, dx \quad (4)$$

The Fortran code *MAMOUT* is specially devoted to the numerical resolution of Eq. 3. It can handle planar, cylindrical or 3D Cartesian geometries. Three models of fluids are presently implemented: incompressible fluid, perfect gas and chemical equilibrium mixture described by a tabulated Mollier diagram. The program manages automatically the processing of a series of boundary-layer profiles, with a double sweep on a frequency range and on ψ angle. An example of computation of Mack's mode amplification on a cone with rigid or porous wall can be found in reference [1], with comparisons between *MAMOUT* and DNS results. An extension to chemical nonequilibrium mixtures of reacting gases is presently under progress.

For cases where the crosswise variation of the mean flow can no longer be neglected, a different ansatz must be used, with two-dimensional eigenfunctions:

$$q'(x,y,z,t) = \hat{q}(y,z)\exp[i(\alpha x - \omega t)] \quad (5)$$

The eigenvalue problem still corresponds to Eq. 3 but the matrices A and B are now larger. This approach can be named LST-2D or bilocal. The name BiGlobal is sometimes used also but it may create a confusion with global stability analysis in the streamwise direction, whereas the present approach concerns a cross-stream plane and is therefore local in the streamwise direction.

The Fortran code *BIGSAM* can address LST-2D problems for incompressible fluid or perfect gas. It has been successfully applied by Lefieux *et al.* [2] to the stability analysis of a cross-stream vortex generated by a hypersonic boundary layer past an isolated roughness on a flat plate. The amplification predicted by LST-2D compares reasonably well with DNS results.

2.3. Parabolized stability equations

Whereas in the frame of local stability analysis the streamwise gradients of the base flow are neglected, a better level of approximation can be obtained with the Parabolized Stability Equations (PSE). Now the *x*-derivatives of the base flow and of the wave number α are taken into consideration. Only the second-order *x*-derivatives are neglected. For PSE-2D, a Fourier transform is still applied on the crosswise coordinate *z*. A modified ansatz is used:

$$q'(x,y,z,t) = \hat{q}(x,y)\exp[i(\int_0^x \alpha(x)dx + \beta z - \omega t)] \quad (6)$$

The main difference with Eq. 2 is the dependency of both the shape function $\hat{q}$ and the oscillatory exponential term on the streamwise coordinate *x*. The idea is that the fast oscillations of the wave are contained in the exponential term whereas the slow variations due to the axial evolution of the base flow are included in the shape functions. This can be achieved through a normalization condition such as:

$$\int_0^\infty q^* \frac{\partial q}{\partial x} dy = 0 \tag{7}$$

This condition must be solved by iteration on α, together with the system obtained by reporting Eq. 6 into the linearized Navier-Stokes equations. In spite of their name, the PSE are not fully parabolic, however they can be solved by forward marching, taking into account some restrictions on the step size. A local eigenmode is usually taken as initial condition at the upstream station. The PSE offer a fast and costless manner to improve the results of the strictly local stability approach for the description of the most unstable mode in a boundary-layer or in a jet shear-layer, for example.

Another Fortran code named *PASTEQ* solves the PSE-2D in curvilinear coordinates for different geometries. To simplify the pre-processing, the base flow is provided in Cartesian coordinates. Incompressible fluid, perfect gas or chemical equilibrium gas mixture are presently available.

Some results of PSE computations on a cone are plotted in Fig. 1, together with LST results. It corresponds to a generic cone with 7° half angle, 1.1 m length and 2.5 mm nose radius tested in JAXA's shock tube HIEST [3]. The Mach number is about 7.7 and the stagnation enthalpy is 3.2 MJ/kg. With a cold wall assumed at 300 K, the temperature inside the boundary layer does not exceed 1500 K except close to the nose and therefore, a perfect gas hypothesis can be assumed for stability computations. The instability found corresponds to Mack's second mode, where the most amplified waves are parallel to the *x*-axis (β = 0), at very high frequencies, requiring special sensors such as PCB to be recorded during the tests. Knowing the transition location, observed in the experiment near x = 0.8 m, will provide the value of N_T for this facility. In the present case, both approaches give rather similar results but the PSE predict a slightly lower amplification level.

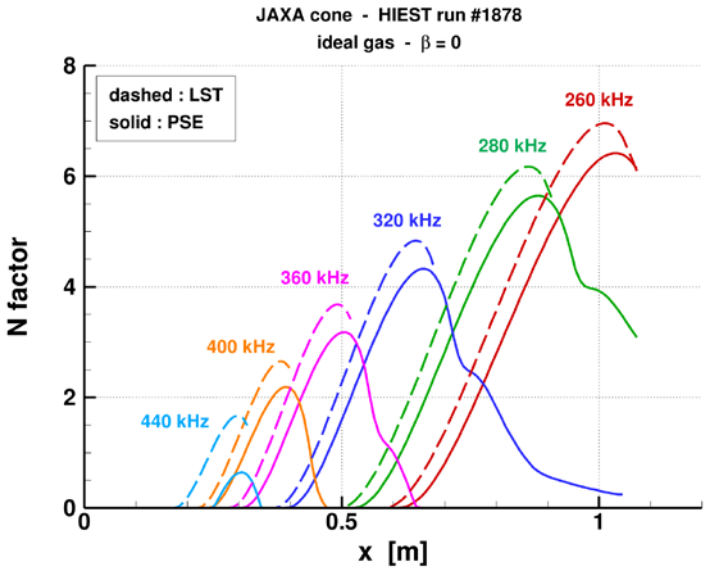

Fig. 1 N factor on a 7° cone in HIEST at Mach 7.8

When the dependency of the base flow on the crosswise coordinate *z* can no longer be neglected, three-dimensional shape functions can be used, with slow variation along *x* and strong variations along *y* and *z*, according to the following ansatz:

$$q'(x,y,z,t) = \hat{q}(x,y,z)\exp[i(\int_0^x \alpha(x)dx - \omega t)] \tag{8}$$

The PSE-3D are still solved by forward marching along *x* but now the shape functions must be solved at each station in a cross-stream plane.

An extension of *PASTEQ* code is planned to solve PSE-3D, first for incompressible fluids, then later for perfect gases. This capability will be useful to study instabilities in the wake of an isolated roughness and to try to improve the results provided by LST-2D. Other configurations such as a cone with an angle of attack or a non-circular cone are also in the range of application of PSE-3D.

2.4. Other methods

Both LST and PSE approaches rely upon the hypothesis of slowly varying mean flow in the streamwise direction. When this is no longer the case, for example when the wall exhibits an indentation such as an angle, a step or a gap, the concept of axial wave number is no longer relevant in the neighbouring of the indentation. Then a global stability analysis must be performed, where all the domain must be considered globally. Such tools are developed at ONERA DAAA, located in Meudon centre, near Paris. These tools are based in particular on the resolvent theory, and they have shown very powerful capacity to analyse the instability of a separated bubble caused by shock wave/boundary layer interaction on a ramp [4,5]. Similar approaches are also called Input/Output analysis in USA.

However, these methods require a lot of computational resources to compute singular values of large matrices and they are not suitable for parametric studies where a large number of configurations must be processed. Therefore a more simple approach has emerged for about a decade, called Harmonic Linearized Navier-Stokes equations (HLNS). The whole fluid domain is considered globally but instead of seeking global eigenmodes, the forced response to an harmonic perturbation imposed at the domain inlet will be computed. Discretizing the linear Navier-Stokes equations in the frequency domain, the resolution only requires to solve a linear system A.X = B, which can be done efficiently with parallel linear algebra libraries. Attention must be paid to apply a suitable non-reflecting boundary condition at the domain outlet.

3. Transition modelling on a smooth surface

When computing a steady RANS solution on any kind of body, it is necessary to estimate the position of the laminar-turbulent transition, downstream of which the turbulence model must be activated. Even the basic LST-1D presented above is too computationally expensive to be directly included into a RANS solver. Moreover, stability computations often require human control and are difficult to fully automate. Semi-empirical transition models were therefore early developed to provide a fast estimate of the transition location.

The first transition model developed at ONERA by Arnal, Habiballah and Delcour in 1984 was the AHD criterion, devoted to streamwise instability of Tollmien-Schlichting waves [6]. It was later extended first to Mach 1.6 and recently up to Mach 4 [7], taking into consideration the fact that for supersonic flows the most unstable waves are no longer streamwise but oblique waves. AHD4 is a piecewise analytical criterion taking into account only Mack's first mode, which generate an estimate of a transition Reynolds number in a way similar to AHD. AHD4 also contains a wall temperature correction. Additional work is under progress to reach Mach 8 with a new criterion named JP8 [8].

To derive these longitudinal criteria, a family of boundary-layer profiles was generated from compressible Falkner-Skan locally self-similar solutions, indexed by the four parameters [M_e, T_{ie}, T_w/T_f, Λ_2], where M_e and T_{ie} are respectively the Mach number and the stagnation temperature at the boundary-layer edge, T_w is the wall temperature, T_f is the temperature which would be obtained on an adiabatic wall, and Λ_2 is the Pohlhausen parameter defined by

$$\Lambda_2 = \frac{\rho_e \theta^2}{\mu_e} \frac{dU_e}{dx} \tag{9}$$

This parameter represents the streamwise velocity (or pressure) gradient. For high Mach numbers, it can be superseded by the parameter $C_f/2\ R_\theta$. Then stability computations were performed with the standard local approach. The amplification was then modelled by a simple linear relation:

$$\text{for } R_\theta > R_{\theta cr}\text{: } N = A\,(R_\theta - R_{\theta 0}) \tag{10}$$

where the critical Reynolds number $R_{\theta cr}$, the slope $A = \frac{dN}{dR_\theta}$ and the parameter $R_{\theta 0}$ are computed by analytical fits or interpolation on the four parameters defining the self-similar solutions. Eq. 10 can be

used inside a RANS solver to estimate the local N factor, knowing the local boundary-layer parameters.

Above Mach 5, the Tollmien-Schlichting instability, labelled as first mode, is overtaken by Mack's second mode, with a higher streamwise amplification. Based on lookup tables, the JP8 model integrates the contributions of both first and second modes, via an envelope method, and it provides an estimation of the local N factor, representing the global amplification of the perturbations. The initial formulation is limited to adiabatic wall conditions, but work started taking into account a cold wall condition with good prospects. The Fig. 2 shows a comparison of Reynolds numbers $R_{\theta T}$ at transition location, provided by the previous AHD4 criterion, the new JP8 criterion, and local linear stability computations, for a boundary layer developing past an adiabatic flat plate at a constant Mach number between 0 and 8. In this case, without pressure gradient, the boundary layer is really self-similar and the JP8 model behaves satisfactorily. The slope break beyond Mach 6 is due to the predominance of the second mode.

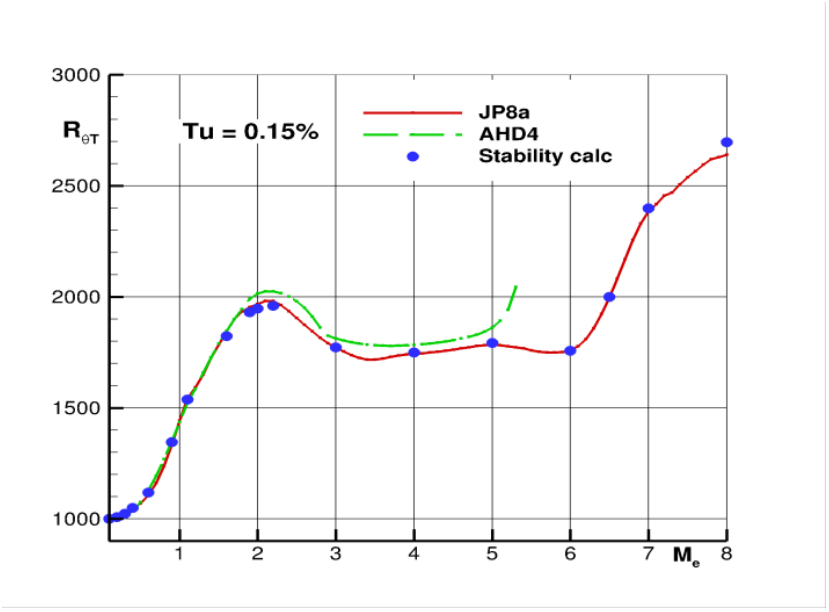

Fig. 2 Transition prediction on a smooth flat plate

Then the effect of the streamwise velocity gradient was investigated, for three different Mach numbers. The synthetic boundary layer profiles deduced from self-similar solutions were completed by true solutions of the Prandtl boundary-layer equations computed with the same velocity gradient as the self-similar solution at the boundary-layer edge. The wall was still assumed adiabatic. Both solutions provide identical flow in the final section but the main difference is that the Prandtl solutions take into account the streamwise gradient of the Mach number, fixed by the isentropic equation in the inviscid flow, whereas the self-similar solutions assume a constant Mach number outside of the boundary layer. The flow history is thus different. Both boundary layer solutions were submitted to local stability analysis. The results are summarised in Fig. 3 where the slope (representing the local growth rate) is plotted as function of the Pohlhausen parameter. The three criteria AHD low speed, AHD Mach 1.6 and AHD Mach 4 are compared to the exact amplifications computed on the basis of the self-similar profiles and on the Prandtl solutions. Computations have been made at Mach 0.2, 1.1 and 2.5. All the AHD models reproduce rather correctly the stability computations based on the self-similar profiles, except at Mach 0.2 for high positive values of the velocity gradient. At Mach 0.2, the flow is really self-similar and the effect of the Mach number is weak (incompressible regime). Therefore the stability computations based on self-similar solutions are very close to the results based on Prandtl solutions. At Mach 1.1 and 2.5, the AHD models agree with the stability computations based on the Prandtl solutions for moderate values of the Pohlhausen parameter, but the agreement range is seen to decrease when the Mach number increases: some discrepancies between self-similar and Prandtl solutions already appear at Mach 2.5 for negative velocity gradients.

The conclusion that can be drawn from the above result is that the AHD-type models are rather powerful for moderate supersonic flows but that the direct extension to higher Mach numbers induces

some systematic errors for large positive or negative velocity gradients. A reflection is under progress to find how to improve the models in this case. However, many hypersonic vehicles have surfaces with low streamwise curvature, except in the nose region where the transition is not likely to occur. Thus the existing criteria can nevertheless be helpful, if used carefully.

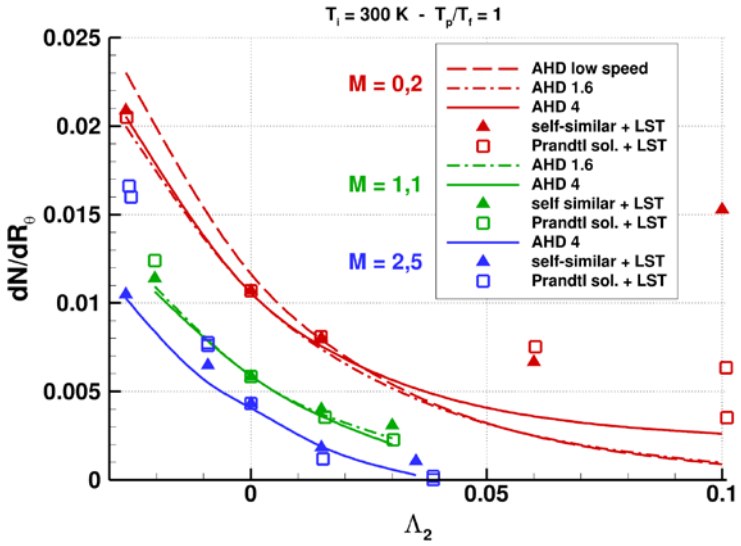

Fig. 3 N factor slope estimate with positive or negative pressure gradient

4. Effect of a transverse gap on the transition location

The role of surface imperfections on transition location has also been the subject of several experimental and theoretical works at ONERA. The effect of a transverse gap on a two-dimensional boundary layer has been particularly investigated. The selected geometry is a flat plate with a rectangular gap. A series of flow configurations has been selected, varying the gap size and aspect ratio with regard to the boundary-layer thickness. A first model named ΔN was derived for subsonic flows, based on local linear stability computations [9]. The model provides two quantities: N_{peak} and ΔN_{far} (Fig. 7). The first one represents an estimation of the N factor value at the gap abscissa. If this parameter exceeds the prescribed N_T value, transition occurs immediately above the gap. Otherwise, the N factor value downstream of the gap will be the sum of the N factor on an equivalent smooth plate plus ΔN_{far}. In this way the transition is seen to move upstream gradually. This model was compared with experimental data. The same approach has been also applied to forward- or backward-facing steps.

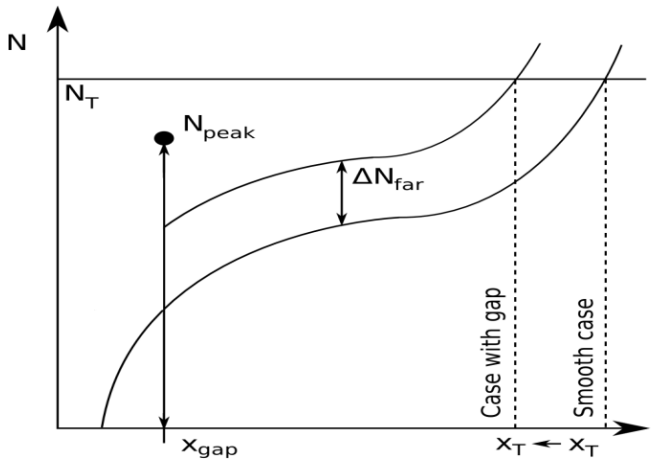

Fig. 4 Effect of a transverse gap on transition location

An improved approach, based no longer on local stability but on two-dimensional harmonic linearized Navier-Stokes solutions, has been recently developed. It provides a better evaluation of the global amplification of an oncoming wave past the gap. The principle is shown in Fig. 5. The HLNS equations are solved in a two-dimensional domain above the gap. A local Tollmien-Schlichting eigenmode at a suitable frequency is imposed as forcing source at the domain inlet. Fig. 6 shows an example of solution, for the axial velocity component, in a generic low-speed case. The oncoming TS wave is strongly perturbed by the gap but downstream the TS wave is recovered with a larger amplitude. The corresponding N factor is plotted in Fig. 7, together with the N factor obtained on a smooth plate and the ΔN. The N factor is seen to undergo a strong increase above the gap, due to high frequency inflectional instabilities in the shear layer. But at the gap trailing edge there is a sudden decrease in the fluctuation amplitude, which cannot be predicted by purely local stability analysis.

In this way, the accuracy of the existing ΔN model can be improved. A new model based on parametric HLNS computations coupled with a neural network has just been developed [11]. This promising approach is up to now limited to incompressible flows but the extension to compressible flows will be undertaken in the near future. In this way it could be possible to address the problem of transition triggering by gaps between thermal protection tiles on re-entry vehicles.

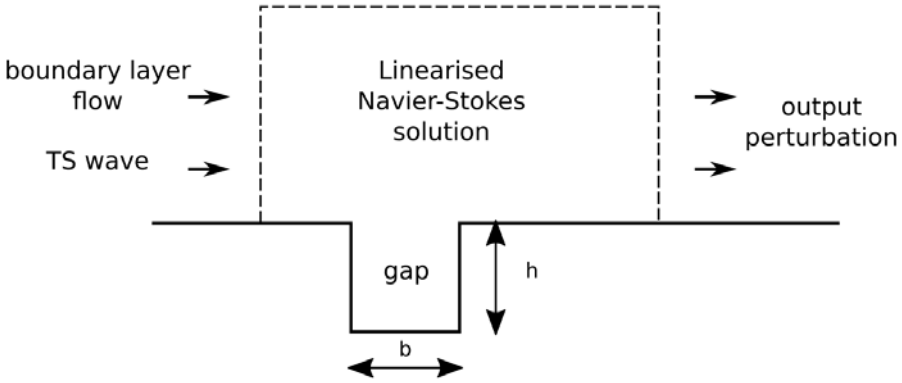

Fig. 5 HLNS computational domain

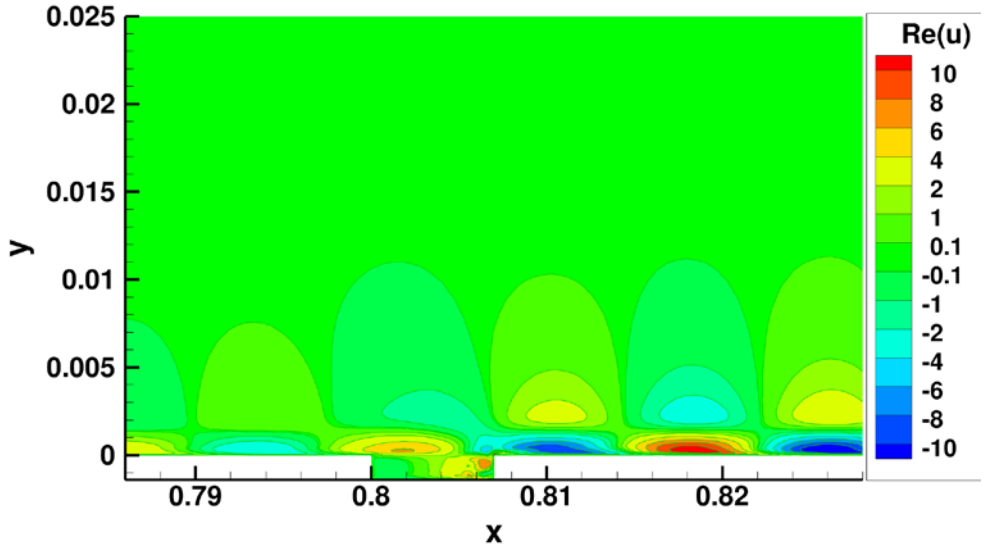

Fig. 6 Axial velocity fluctuation past a gap, computed with HLNS

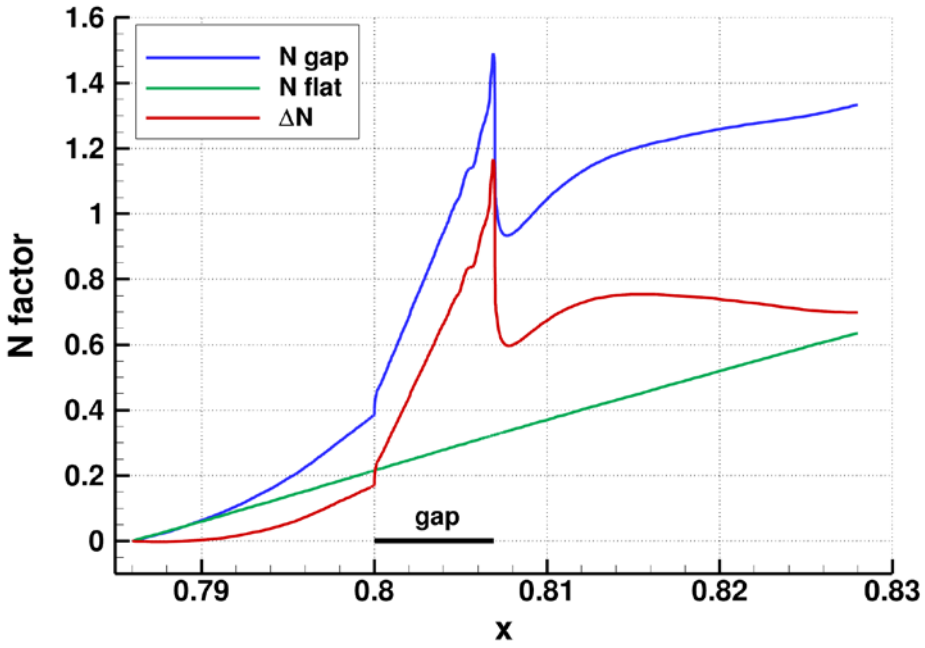

Fig. 7 N factor evolution past a gap, computed with HLNS

References

1. Fiévet, R., Deniau, H., Brazier, J.-Ph., and Piot, E.: Numerical analysis of porous coatings stabilizing capabilities on hypersonic boundary-layer transition. AIAA Journal 59 (10) 3845–3858 (2021)
2. Lefieux, J., Garnier, E., Brazier, J.-Ph., Sandham N., and Durant, A.: Roughness-induced instabilities and transition on a generic hypersonic forebody at Mach 6. AIAA Journal 59 (9) 3529–3545 (2021)
3. Matsuse, Y., Saijo, M., Ishihara, T., Ogino, Y., Ohnishi, N., and Tanno, H.: Global stability analysis on cone models under the conditions of the HIEST experiments. AIAA Paper 2016-0956, 54th AIAA Aerospace Sciences Meeting, San Diego (2016)
4. Lugrin, M., Beneddine, S., Leclercq, C., Garnier, E., and Bur, R.: Transition scenario in hypersonic axisymmetrical compression ramp flow. Journal of Fluid Mechanics 907, A6 (2021)
5. Lugrin, M., Beneddine, S., Garnier, E., and Bur, R.: Multi-scale study of the transitional shock-wave boundary layer interaction in hypersonic flow. Theoretical and Computational Fluid Dynamics 36, 277–302 (2022)
6. Arnal, D., Habiballah, M., and Coustols, E.: Laminar instability theory and transition criteria in two and three-dimensional flow. La Recherche Aérospatiale n°2, 45–63 (1984)
7. Perraud, J., and Durant, A.: Stability-based Mach zero to four longitudinal transition prediction criterion. Journal of Spacecraft and Rockets 53 (4), 730–742 (2016)
8. Perraud, J., and Brazier, J.-Ph.: Mach 0 to 8 transition criterion for a 2D flow of ideal gas. International Conference on Flight Vehicles, Aerothermodynamics and Re-entry Missions & Engineering, FAR 2019, Monopoli (2019)
9. Beguet, S., Perraud, J., Forte, M., and Brazier, J.-Ph.: Modeling of transverse gaps effects on boundary-layer transition. Journal of Aircraft 54 (2), 794–801 (2017)
10. Methel, J., Forte, M., Vermeersch, O., and Casalis, G.: An experimental study on the effects of two-dimensional positive surface defects on the laminar-turbulent transition of a sucked boundary layer. Experiments in Fluids 60 (6) 94 (2019)

11. Rouviere, A., Pascal, L., Méry, F., Simon, E., and Gratton, S.: Neural prediction model for transition onset of a boundary-layer in presence of 2D surface defects. AIAA Paper 2022-1073, AIAA SciTech 2022 Forum, San Diego (2022)